

# Coherent Control of Magneto-optical Rotation in Inhomogeneously Broadened Medium

Anil K. Patnaik\* and G. S. Agarwal

*Physical Research Laboratory, Navrangpura, Ahmedabad-380 009, India*  
(October 24, 2018)

We extend our earlier investigations [Opt. Commun. **179**, 97 (2000)] on the enhancement of magneto-optical rotation (MOR) to include inhomogeneous broadening. We introduce a control field that counter-propagates with respect to the probe field. We derive analytical results for the susceptibilities corresponding to the two circular polarization components of the probe field. From the analytical results we identify and numerically demonstrate the region of parameters where significantly large magneto-optical rotation (MOR) can be obtained. From the numerical results we *isolate* the significance of the magnetic field and the control field in enhancement of MOR. The control field opens up many new regions of the frequencies of the probe where large magneto-optical rotation occurs. We also report that a large enhancement of MOR can be obtained by operating the probe and control field in two-photon resonance condition.

PACS no. 42.50.Gy, 33.55.Ad, 42.25.Lc

## I. INTRODUCTION

A magnetic field, when applied to an initially isotropic medium containing gaseous atoms having  $m$ -degenerate sublevels, can cause birefringence in the medium. Because, the applied magnetic field creates asymmetry between the susceptibilities  $\chi_{\pm}$  of the medium corresponding to the two circularly polarized components  $\sigma_{\mp}$  of the probe field. That results in magneto-optical rotation (MOR), i.e. the plane of polarization of a weak probe field is rotated when it passes through the medium. For a small absorption the rotation angle  $\theta$  is given by

$$\theta = \pi k_p l (\chi_- - \chi_+) ; \quad (1)$$

where  $\vec{k}_p$  corresponds to propagation vector of the probe and  $l$  is length of the cell along  $\vec{k}_p$ . Further we note that,  $\chi_{\pm}$  depend on the atomic density and the oscillator strength of the atomic transition.

Traditionally MOR was used as a tool in polarization spectroscopy using continuum sources [1]. The interest in MOR was intensified in the atomic and molecular physics with the availability of intense light sources of definite polarization [2] and frequency [3]. Several reviews exist in the literature on this subject including several interesting applications (e.g., see [4]). Using saturating fields the non-linear MOR has also been studied at length [5–8]. MOR with a transverse magnetic fields [9] (known as Voigt effect) and with inclined magnetic fields [10] have also been studied. Recently large MOR has been reported in dense and cold atomic cloud of Rubidium [11]. On the other hand, laser field *alone* can also break the symmetry in the response of an atomic gas to different polarization components of a probe field. For example, let us consider  $j = 0 \leftrightarrow j = 1$  transitions of an atomic gas containing  $V$  systems. When a linearly polarized weak probe field passes through the medium, the  $\sigma_{\pm}$  components of the probe field couple the  $|j = 0, m = 0\rangle$  with the degenerate states  $|j = 1, m = \mp 1\rangle$ . The susceptibilities  $\chi_{\pm}$  of the medium to these two components  $\sigma_{\mp}$  are same; i.e., response of the medium is symmetric to both the components. However when a  $\sigma_-$  polarized strong field is applied on the  $|j = 0, m = 0\rangle \leftrightarrow |j = 1, m = 1\rangle$  transition, the susceptibility  $\chi_+$  is modified by the control field parameters creating asymmetry between  $\chi_+$  and  $\chi_-$ . Thus the plane of polarization of the probe field rotates (due to Eq. (1)). Note that, this rotation is solely due to the laser field and is a function of control field parameters. Resonant birefringence due to optically induced level shift by a coherent source was observed [12]. The light-induced polarization rotation in optical pumping experiments with incoherent light has also been extensively studied [13]. Liao and Bjorklund [14] were the first to observe polarization rotation in a three level system by resonant enhancement of two-photon dispersion in the  $3s^2S_{1/2} \leftrightarrow 5s^2S_{1/2}$  of sodium vapor. Hänch and coworkers [15] have used this polarization rotation as a high resolution spectroscopic technique. Heller *et al* [16] extended this idea to atomic

---

\*Present Address: Department of Applied Physics and Chemistry, University of Electro-Communications, Chofu, Tokyo 182-8585, Japan

systems involving the ionization continuum. Experimental and theoretical work has been reported by Ståhlberg *et al* [17] on laser induced dispersion in a three level cascade system of *Ne* discharge.

Recently, combining the ideas of enhancement of refractive index using atomic coherence [18] and the non-linear MOR, Scully and his coworkers have investigated a possible application to high-precision optical magnetometry [19,20]. They have demonstrated this possibility both theoretically [19] and experimentally [20], considering the rotation of polarization of a strong linearly polarized probe caused by an optically thick cell containing  $^{87}\text{Rb}$  vapor. The maximum sensitivity reported in their experiment is  $\sim 6 \times 10^{-12}\text{Gauss}/\sqrt{\text{Hz}}$ , which is superior to other existing high precision magnetometers. Budker *et al* at Berkeley have also reported high sensitive optical magnetometry in a series of papers [21], based on the non-linear MOR involving ultra-narrow resonances ( $\simeq 2\pi \times 1.3\text{Hz}$ ) using special cell with high quality anti-relaxation paraffin coating that enables the atomic coherence to survive even after a large number of collisions with the wall. Using a similar configuration, Budker *et al* have shown reduction of the group velocity of light to  $\simeq 8\text{ m/sec}$  in a non-linear magneto-optical system [22]. Further, Pavon *et al* [23] introduced the idea of *coherent control* to obtain significant atomic birefringence in presence of electromagnetically induced transparency (EIT) [24]. Winelandy and Gaeta [25] used quantum coherence to control the polarization state of a probe field. They reported a large birefringence and hence a large polarization rotation in a three-level cascade of  $^{85}\text{Rb}$  (see also [26,27]). Using a similar configuration, Fortson and coworkers [28] have showed a possible utility of the polarization rotation at EIT to measure the atomic parity non-conservation signal with a better efficiency. A detailed discussion on the role of degenerate sublevels and effect of the polarized fields on EIT has been discussed in [29].

However, it is interesting to investigate the combined effects of the laser field and the magnetic field in the context of *coherent control* of the rotation of polarization. In our earlier work [26], we have reported laser field induced enhancement of MOR in *cold* atoms. In the present paper we generalize the above work [26] by including the thermal motions of the atoms inside the cell (see Fig. 1). Here a large broadening is introduced in the rotation signal. This could be desirable to get large rotations for a broad range of probe frequencies in presence of a control field. But on the other hand, broadening reduces the magnitude of rotation considerably. However, one can work with a denser medium when Doppler effect is included in the calculation. Moreover, we have included *all spontaneous decay events* involved in the  $j = 0 \rightarrow j = 1 \rightarrow j = 0$  transitions of the system (unlike in [26]). Further we discuss a special case when the weak probe field and strong control field are in two-photon resonance with  $|e\rangle \leftrightarrow |g\rangle$  transition, that gives rise to large enhancement of MOR.

The organization of the paper is the following. In Sec. II, we describe the model scheme and determine the susceptibility of a moving atom using density matrix formalism. In Sec. III, we present the analytical results for the susceptibilities of the Doppler broadened medium. In Sec. IV, we give a measure of rotation of plane of polarization. In Sec.V, we show how one identifies the regions of interest by suitably choosing the control field parameters. In Sec. VI, we present numerical results that substantiates the analytical results. We show that indeed large MOR could be obtained due to the control field. We analyze different probe frequency regions to understand the contributions of electric and magnetic field to the large polarization rotation. In Sec. VI, we discuss a special case where the counter propagating probe and control field are in two-photon resonance with the  $|e\rangle \leftrightarrow |g\rangle$  transition (see Fig. 2). We show both analytically and numerically that this configuration can be advantageous for enhancement of MOR. We conclude with a summary of the results in Sec.VII.

## II. THE MODEL AND THE SUSCEPTIBILITIES

The MOR consists of the propagation of linearly polarized light  $\vec{E}_p$  tuned close to the transition  $j \leftrightarrow j'$  in presence of a magnetic field  $\vec{B}$ . The susceptibilities  $\chi_{\pm}$  for the two circularly polarized components of the probe beam would be different as  $\vec{B} \neq 0$ . We can now consider coherent control of MOR in a configuration as depicted in Fig. 1 with a control field  $\vec{E}_c$  which can be tuned close to another transition say  $j' \leftrightarrow j''$ . The atoms move randomly inside the cell with velocity  $\vec{v}$ . The probe field  $\vec{E}_p$  and control field  $\vec{E}_c$  are taken to be counter propagating. The model scheme we consider (Fig. (2)) is a generalization of the scheme in [26]. Here we have included the spontaneous decays between  $m = 0 \leftrightarrow m = 0$  states in the calculation, which was neglected in [26]. The decay coefficients corresponding to  $|e\rangle \rightarrow |i\rangle$  ( $|i\rangle \rightarrow |g\rangle$ ) transitions are denoted by  $2\Gamma_i$  ( $2\gamma_i$ ). In what follows below, we outline the calculation of susceptibilities of the atoms, moving at  $\vec{v}$ , to the  $\sigma_{\pm}$  components of the probe field.

We write the fields in the circular basis as

$$\vec{E}_{\alpha} = (\mathcal{E}_{\alpha+}\hat{\epsilon}_{+} + \mathcal{E}_{\alpha-}\hat{\epsilon}_{-}) e^{i\vec{k}_{\alpha}\cdot\vec{r} - i\omega_{\alpha}t}, \quad \alpha = c, p; \quad (2)$$

where

$$\hat{\epsilon}_{\pm} = \frac{\hat{x} \pm i\hat{y}}{\sqrt{2}}. \quad (3)$$

Here  $\mathcal{E}_{c\pm}$  ( $\mathcal{E}_{p\pm}$ ) represent the  $\sigma_{\mp}$  components of the control field (probe field). Let the dipole matrix elements corresponding to  $|e\rangle \leftrightarrow |i\rangle$  and  $|i\rangle \leftrightarrow |g\rangle$  transitions be represented by  $\vec{D}_{ei}$  and  $\vec{d}_{ig}$  respectively. The polarization state of the incident fields decide the various field couplings between the  $j = 0 \leftrightarrow j = 1 \leftrightarrow j = 0$  states. The dipole matrix elements  $\vec{D}_{ij}$  and  $\vec{d}_{ij}$  can be written with their corresponding Clebsch-Gordan coefficients as

$$\begin{aligned}\vec{D}_{e1} &= -D\hat{\epsilon}_+, \quad \vec{D}_{e2} = D\hat{\epsilon}_-, \\ \vec{d}_{1g} &= -d\hat{\epsilon}_-, \quad \vec{d}_{2g} = d\hat{\epsilon}_+\end{aligned}\quad (4)$$

where  $D$  ( $d$ ) denotes the reduced dipole matrix element corresponding to upper (lower)  $j = 0 \leftrightarrow j = 1$  ( $j = 1 \leftrightarrow j = 0$ ) transitions.

In the rotating wave approximation, the interaction Hamiltonian  $\mathcal{H}_I$  corresponding to the scheme in Fig. 2 is

$$\mathcal{H}_I(t) = -\hbar \sum_{i=1,2} \left[ |i\rangle\langle g|g_i e^{-i\omega_p t + i\vec{k}_p \cdot \vec{v}t} + |e\rangle\langle i|G_i e^{-i\omega_c t + i\vec{k}_c \cdot \vec{v}t} + H.c. \right]; \quad (5)$$

where Rabi frequencies  $2G_i$  and  $2g_i$  of the control and probe lasers are

$$G_i = \frac{\vec{D}_{ei} \cdot \vec{\mathcal{E}}_c}{\hbar}, \quad g_i = \frac{\vec{d}_{ig} \cdot \vec{\mathcal{E}}_p}{\hbar}. \quad (6)$$

On combining Eq.(4) and (6) we obtain,

$$\begin{aligned}G_1 &= -\frac{D\mathcal{E}_{c-}}{\hbar}, \quad G_2 = \frac{D\mathcal{E}_{c+}}{\hbar}, \\ g_1 &= -\frac{d\mathcal{E}_{p+}}{\hbar}, \quad g_2 = \frac{d\mathcal{E}_{p-}}{\hbar}.\end{aligned}\quad (7)$$

In terms of Fig. 2, the unperturbed Hamiltonian  $\mathcal{H}_0$  is

$$\mathcal{H}_0 = \hbar(\omega_{eo} + \omega_{og})|e\rangle\langle e| + \hbar(\omega_{og} + \zeta)|1\rangle\langle 1| + \hbar\omega_{og}|o\rangle\langle o| + \hbar(\omega_{og} - \zeta)|2\rangle\langle 2|. \quad (8)$$

Here  $\hbar\omega_{eo}$  ( $\hbar\omega_{og}$ ) is the energy separation between  $|e\rangle$  ( $|g\rangle$ ) and  $|o\rangle$ , and  $2\zeta = \mu_B B/\hbar$  is the Zeeman splitting of the degenerate levels, caused by the magnetic field  $B$ . The atomic dynamics is described by the master equation

$$\dot{\rho} = \frac{-i}{\hbar}[\mathcal{H}_0 + \mathcal{H}_I(t), \rho] - \sum_{i=o,1,2} (\Gamma_i\{|e\rangle\langle e|, \rho\} + \gamma_i\{|i\rangle\langle i|, \rho\} - 2\Gamma_i\rho_{ee}|i\rangle\langle i| - 2\gamma_i\rho_{ii}|g\rangle\langle g|). \quad (9)$$

The second term under the summation sign represents the natural decays of the system. The curly bracket represents the anti-commutator. The explicit time dependence can be eliminated by making a transformation  $\rho \rightarrow \tilde{\rho}$  such that

$$\begin{aligned}\tilde{\rho}_{ii} &= \rho_{ii}, \quad \tilde{\rho}_{ig} = \rho_{ig} e^{i\omega_p t - i\vec{k}_p \cdot \vec{v}t}, \\ \tilde{\rho}_{ei} &= \rho_{ei} e^{i\omega_c t - i\vec{k}_c \cdot \vec{v}t}, \quad \tilde{\rho}_{eg} = \rho_{eg} e^{i(\omega_p + \omega_c)t - i(\vec{k}_p + \vec{k}_c) \cdot \vec{v}t}.\end{aligned}\quad (10)$$

The matrix equation for  $\tilde{\rho}$  is found to be

$$\dot{\tilde{\rho}} = \frac{-i}{\hbar}[\mathcal{H}_{\text{eff}}, \tilde{\rho}] - \sum_{i=o,1,2} (\Gamma_i\{|e\rangle\langle e|, \tilde{\rho}\} + \gamma_i\{|i\rangle\langle i|, \tilde{\rho}\} - 2\Gamma_i\tilde{\rho}_{ee}|i\rangle\langle i| - 2\gamma_i\tilde{\rho}_{ii}|g\rangle\langle g|), \quad (11)$$

with the effective Hamiltonian in the transformed frame

$$\begin{aligned}\mathcal{H}_{\text{eff}} &= \hbar(\delta_v + \Delta_v)|e\rangle\langle e| + \hbar(\delta_v + \zeta)|1\rangle\langle 1| + \hbar(\delta_v - \zeta)|2\rangle\langle 2| \\ &\quad - \hbar \sum_{i=1,2} (g_i|i\rangle\langle g| + G_i|e\rangle\langle i| + H.c.); \end{aligned}\quad (12)$$

where

$$\delta_v = \delta + k_p v_z, \quad \Delta_v = \Delta - k_c v_z. \quad (13)$$

Here  $\delta = \omega_{og} - \omega_p$ ,  $\Delta = \omega_{eo} - \omega_c$  correspond to the detunings of the probe and control field when the atom is stationary. Further we assume  $k_p \approx k_c$  for simplicity. Thus one can write

$$\Delta_v + \delta_v \approx \Delta + \delta. \quad (14)$$

Here it may be noted that due to our particular choice of counter propagating probe and control fields, the two-photon resonant terms can be made independent of atomic velocity [See e.g. in Eq. (20)]. The configuration consisting of counter propagating probe and control field in ladder system has been shown to be useful in Doppler free polarization spectroscopy [15], EIT [30] and LWI [31].

Let  $\chi_+$  ( $\chi_-$ ) be the susceptibilities of the moving atom corresponding to the  $\sigma_-$  ( $\sigma_+$ ) component of the probe field. We choose the probe field polarization such that  $g_i \neq 0$ . One can write  $\chi_{\pm}$  in terms of dimensionless quantities as

$$\chi_{\pm} = \left( \frac{\alpha}{4\pi k_p} \right) s^{\pm}; \quad (15)$$

where  $s^{\pm}$ , the normalized susceptibilities are given by

$$s^+ = \left( \frac{\tilde{\rho}_{1g}\gamma}{g_1} \right), s^- = \left( \frac{\tilde{\rho}_{2g}\gamma}{g_2} \right). \quad (16)$$

Here  $\alpha l$  is weak probe field absorption at the line center and is given by  $\alpha l = 4\pi k_p l |d|^2 n / (\hbar \gamma)$ ; where  $n$  denotes the atomic density and  $l$  is the length of the cell. For simplicity, we assume  $\gamma_1 = \gamma_2 = \gamma_o = \gamma$ . Under steady state conditions, we solve Eq. (11) to obtain complete analytical solutions for the susceptibilities  $\chi_{\pm}$  or the normalized susceptibilities  $s^{\pm}$

$$s^+ = \frac{i\gamma [ |G_2|^2 + (\gamma + i(\delta_v - \zeta))(\Gamma_o + \Gamma_1 + \Gamma_2 + i(\Delta_v + \delta_v)) ]}{|G_2|^2(\gamma + i(\delta_v + \zeta)) + (\gamma + i(\delta_v - \zeta)) [ |G_1|^2 + (\gamma + i(\delta_v + \zeta))(\Gamma_o + \Gamma_1 + \Gamma_2 + i(\Delta_v + \delta_v)) ]}, \quad (17)$$

$$s^- = \frac{i\gamma [ |G_1|^2 + (\gamma + i(\delta_v + \zeta))(\Gamma_o + \Gamma_1 + \Gamma_2 + i(\Delta_v + \delta_v)) ]}{|G_1|^2(\gamma + i(\delta_v - \zeta)) + (\gamma + i(\delta_v + \zeta)) [ |G_2|^2 + (\gamma + i(\delta_v - \zeta))(\Gamma_o + \Gamma_1 + \Gamma_2 + i(\Delta_v + \delta_v)) ]}. \quad (18)$$

In writing (17) and (18), we have used the condition (14). We note that the atomic velocity dependence of  $s^{\pm}$  comes via  $\delta_v$ . The results presented above are susceptibilities of the atoms moving at  $\vec{v}$ , to the lowest order in the probe field. The response of the medium to the input probe field can be obtained by averaging  $s^{\pm}$  over the distribution of velocities. It may be noted that the parameter space in Eqs. (17) and (18) is very large. Therefore we *identify* a particular configuration of our interest and work only in the region which gives large asymmetry between  $\langle s^+ \rangle$  and  $\langle s^- \rangle$  ( $\langle \rangle$  represents average over the velocity distribution of atoms inside the cell), and can lead to large MOR. We focus on a particularly interesting case when  $G_2 = 0$ ; i.e., the control field is  $\sigma_+$ -polarized ( $\mathcal{E}_c \equiv \mathcal{E}_{c-} \neq 0$  and  $\mathcal{E}_{c+} = 0$ ) and it couples to the  $|1\rangle \leftrightarrow |e\rangle$  transition only. Clearly  $s^-$  becomes

$$s^- = \frac{i\gamma}{(\gamma + i(\delta_v - \zeta))}; \quad (19)$$

which is independent of the control field parameters. Whereas  $s^+$  is strongly dependent on the strength and frequency of the control field and is given by

$$s^+ = \frac{i\gamma(\Gamma_o + \Gamma_1 + \Gamma_2 + i(\Delta + \delta))}{|G_1|^2 + (\gamma + i(\delta_v + \zeta))(\Gamma_o + \Gamma_1 + \Gamma_2 + i(\Delta + \delta))}. \quad (20)$$

In absence of the control field, the susceptibilities reduce to

$$s^{\pm} = \frac{\gamma}{((\delta_v \pm \zeta) - i\gamma)}; \quad (21)$$

which clearly indicates that  $s^{\pm}$  are completely symmetric in absence of magnetic field (i.e.  $\zeta = 0$ ). Most of the MOR studies with a weak coherent field use the susceptibility in (21). Further it may be noted that from Eq. (19) and Eq. (20) that,  $s^+ \neq s^-$  even in absence of magnetic field when  $G_1 \neq 0$ . This explains the laser induced birefringence reported by Winelandy and Gaeta [25].

### III. SUSCEPTIBILITIES $\chi_{\pm}$ OF THE DOPPLER BROADENED MEDIUM

Next we calculate the  $\chi_{\pm}$  of a Doppler broadened medium. Here, as mentioned in Sec. II, one needs to average  $s^{\pm}$  over the atomic velocity distribution  $\sigma(v_z)$  inside the cell to obtain the response of the medium

$$\langle s^{\pm} \rangle = \int_{-\infty}^{\infty} s^{\pm}(v_z) \sigma(v_z) dv_z. \quad (22)$$

It is assumed that at thermal equilibrium, the atoms inside the cell follow Maxwell-Boltzmann velocity distribution

$$\sigma(v_z) = (2\pi K_B T / M)^{-1/2} \exp(-M v_z^2 / 2K_B T), \quad (23)$$

where mass of the moving atom is  $M$ , temperature of the cell  $T$  and  $K_B$  is Boltzmann constant. For convenience, transforming the integral in Eq. (22) from velocity space to frequency space [32], we get

$$\langle s^{\pm} \rangle = \int_{-\infty}^{\infty} s^{\pm}(\delta_v) \sigma(\delta_v) d\delta_v, \quad (24)$$

where the distribution in frequency space is

$$\sigma(\delta_v) \equiv \frac{1}{\sqrt{2\pi\omega_D^2}} \exp[-(\delta_v - \delta)^2 / 2\omega_D^2]; \quad \omega_D \simeq \omega_{og} (K_B T / M c^2)^{1/2}. \quad (25)$$

Here  $\omega_D$  represents the Doppler width in frequency space. For our case of  $\sigma_+$  polarized control field, we substitute  $s^{\pm}$  from Eqs. (19) and (20) in Eq. (24) and evaluate the integral. We could obtain the complete analytical results for the Doppler averaged susceptibilities, in terms of complex error functions [33] as

$$\langle s^{-} \rangle \equiv \frac{i\pi\gamma}{\sqrt{2\pi\omega_D^2}} \mathcal{W} \left( \frac{\zeta - \delta + i\gamma}{\sqrt{2}\omega_D} \right); \quad (26)$$

$$\langle s^{+} \rangle \equiv \frac{i\pi\gamma}{\sqrt{2\pi\omega_D^2}} \mathcal{W}(\xi); \quad (27)$$

$$\xi = \frac{1}{\sqrt{2}\omega_D} \left[ i\gamma - \zeta - \delta + \frac{|G_1|^2}{\Delta + \delta - i(\Gamma_o + \Gamma_1 + \Gamma_2)} \right]. \quad (28)$$

The  $\mathcal{W}$  function is defined as

$$\mathcal{W}(z) = \frac{i}{\pi} \int_{-\infty}^{\infty} \frac{e^{-t^2} dt}{z - t}. \quad (29)$$

It can be written in terms of the error function  $\text{Erf}(z)$  as

$$\mathcal{W}(\alpha) = e^{-\alpha^2} (1 - \text{Erf}(-i\alpha)); \quad \text{Erf}(z) = \frac{2}{\sqrt{\pi}} \int_0^z e^{-t^2} dt. \quad (30)$$

It may be noted that the argument of  $\mathcal{W}$  function in  $\langle s^{-} \rangle$  will show usual Doppler profile since it is independent of the control field but the argument of  $\mathcal{W}$  function in  $\langle s^{+} \rangle$  is strongly dependent on the strength and frequency of the control field and therefore, the Doppler profile can be modified with these control field parameters.

### IV. MEASURE OF ROTATION

Using the  $\langle s^{\pm} \rangle$  obtained above, the rotation of polarization  $\theta$  of the probe can be determined from Eq.(1) which, however, is valid only if the absorption of the medium is very small. Since we consider the resonant or near-resonant MOR, one also needs to take into account the large absorption associated with the large dispersions near resonance. Absorption contributes to the polarization rotation via dichroism (rotation solely due to  $\text{Im} \langle s^{\pm} \rangle$ ) but large absorption attenuates the MOR signal at the output.

Let us consider an  $x$ -polarized incident probe field propagating along the quantization axis  $z$ . The field amplitude can be written as

$$\vec{\mathcal{E}}_{in} = \vec{\mathcal{E}}_p(z=0) = \hat{x}\mathcal{E}_0; \quad (31)$$

which can be resolved into two circularly polarized components as

$$\begin{aligned} \vec{\mathcal{E}}_{in} &= \hat{e}_+\mathcal{E}_{p+}(z=0) + \hat{e}_-\mathcal{E}_{p-}(z=0) \\ &= \frac{\mathcal{E}_0}{\sqrt{2}}(\hat{e}_+ + \hat{e}_-). \end{aligned} \quad (32)$$

When the probe field  $\vec{\mathcal{E}}_{in}$  passes through the anisotropic medium,  $\mathcal{E}_{p\pm}(z)$  evolves. In the limit of a weak probe, we get the output field

$$\vec{\mathcal{E}}_{out} = \vec{\mathcal{E}}_p(z=l) = \frac{\mathcal{E}_0}{\sqrt{2}} \left[ \hat{e}_+ e^{i\frac{\alpha l}{2}\langle s^+ \rangle} + \hat{e}_- e^{i\frac{\alpha l}{2}\langle s^- \rangle} \right]. \quad (33)$$

Clearly,  $\vec{\mathcal{E}}_{out}$  contains both  $x$  and  $y$ -polarization components, and thus polarization of the probe is rotated. For small absorption, it is easy to derive the rotation angle  $\theta$  in Eq.(1). Experimentally one observes the rotation by measuring the intensity after passing the output through a crossed polarizer  $P_y$  (as shown in Fig.1) given by

$$T_y = \frac{|(\mathcal{E}_{out})_y|^2}{|\mathcal{E}_{in}|^2} = \frac{1}{4} \left| \exp\left(i\frac{\alpha l}{2}\langle s^+ \rangle\right) - \exp\left(i\frac{\alpha l}{2}\langle s^- \rangle\right) \right|^2; \quad (34)$$

which gives the measure of polarization rotation of the weak  $x$ -polarized probe field. Here the intensity of transmission through  $P_y$ , is scaled with the input intensity in  $x$ -polarization. It should be borne in mind that  $\langle s^\pm \rangle$  are in general complex.

## V. CONDITION FOR ENHANCEMENT OF MOR

In this section we *identify* the regions of our interest. We determine the criteria to choose the control field parameters to efficiently control and hence enhance the MOR. From Eq. (34), one observes the following:

- (i) When  $\langle s^+ \rangle \approx \langle s^- \rangle$ ,  $T_y \rightarrow 0$ .
- (ii) When  $\text{Re} \langle s^+ \rangle \simeq \text{Re} \langle s^- \rangle$  but  $\text{Im} \langle s^+ \rangle \neq \text{Im} \langle s^- \rangle$ ,  $T_y$  reduces to

$$T_y \simeq \frac{1}{4} \left| e^{(-\frac{\alpha l}{2}\text{Im}\langle s^+ \rangle)} - e^{(-\frac{\alpha l}{2}\text{Im}\langle s^- \rangle)} \right|^2. \quad (35)$$

If both  $\frac{\alpha l}{2}\text{Im}\langle s^\pm \rangle$  are large,  $T_y \rightarrow 0$ . However if  $\frac{\alpha l}{2}\text{Im}\langle s^+ \rangle$  is large but  $\frac{\alpha l}{2}\text{Im}\langle s^- \rangle$  is small (or vice versa), we obtain

$$T_y \simeq \frac{e^{\alpha l \text{Im}\langle s^- \rangle}}{4} \rightarrow \frac{1}{4}; \quad (36)$$

which is the rotation due to *dichroism only*.

- (iii) Further when  $\text{Im} \langle s^+ \rangle \approx \text{Im} \langle s^- \rangle = \beta$  (say) but  $\text{Re} \langle s^+ \rangle \neq \text{Re} \langle s^- \rangle$ , we get

$$T_y \simeq \frac{e^{(-\alpha l \beta)}}{4} \left| 1 - e^{i\frac{\alpha l}{2}\text{Re}(\langle s^- \rangle - \langle s^+ \rangle)} \right|^2. \quad (37)$$

If  $\alpha l \beta$  is small,

$$T_y \simeq \frac{1}{4} \left| 1 - e^{i\frac{\alpha l}{2}\text{Re}(\langle s^- \rangle - \langle s^+ \rangle)} \right|^2, \quad (38)$$

thus when

$$\frac{\alpha l}{2}\text{Re}(\langle s^- \rangle - \langle s^+ \rangle) = (2n+1)\pi \quad (n=0, 1, 2, \dots), \quad T_y = 1. \quad (39)$$

This is the *most useful region* for our system. This rotation is solely due to birefringence. However if  $\alpha l \beta$  is large then  $T_y \rightarrow 0$ . This is because a large attenuation of the MOR signal occurs. Thus we have identified that *the most interesting frequency region corresponds to very small value of  $\text{Im}\langle s^\pm \rangle$  and when the asymmetry between  $\text{Re}\langle s^\pm \rangle$  satisfies the condition (39)*. Therefore our objective is to select proper control field parameters so that above condition can be achieved.

## VI. NUMERICAL RESULTS ON COHERENT CONTROL OF MOR

Based on the above observations, we present some interesting numerical results for different parameters to demonstrate the large enhancement of MOR. We define the MOR signal enhancement factor

$$\eta = \frac{(T_y)_{G_1 \neq 0}}{(T_y)_{G_1 = 0}}. \quad (40)$$

For a given  $\delta$ ,  $\eta$  represents the enhancement (if  $\eta > 1$ ) or suppression (if  $\eta < 1$ ) of MOR signal by a control field, when compared to the MOR without control field. We use the notation  $\langle s_0^\pm \rangle$  to represent susceptibilities corresponding to  $\sigma_\mp$  components of the probe when control field is absent and  $\langle s_c^\pm \rangle$  to represent the susceptibility modified by the control field. In the following we give some typical values of various physical parameters used here: the Doppler width  $\omega_D = 50\gamma$  corresponds to  $^{40}\text{Ca}$  cell at a temperature of  $\sim 500\text{K}$ . For length of the cell  $l = 5\text{cm}$ ,  $\alpha l = 300$  corresponds to an atomic density of  $\sim 10^{12} \text{ atoms/cm}^3$ , a Zeeman splitting of  $2\zeta = 20\gamma$  corresponds to a magnetic field of strength  $\sim 200 \text{ Gauss}$ , and  $G_1 = 100\gamma$  would correspond to a laser field of strength  $\sim 5 \text{ W/cm}^2$ .

In Fig. 3, we consider the effect of the control field which is on resonance with the transition  $|e\rangle \leftrightarrow |o\rangle$  (i.e.  $\Delta = 0$ ). We consider density of atoms in the cell such that  $\alpha l = 300$ . We observe significant enhancement of MOR for a large range of probe frequencies. (i) We get the enhancement factor  $\eta = 1.04 \times 10^3$  for  $\delta = 0$ . This can be understood as follows: in the absence of the control field and for  $\delta = 0$ ,  $\text{Im}\langle s_0^+ \rangle = \text{Im}\langle s_0^- \rangle = \beta$  (say) and  $\alpha l \beta$  is large, leading to  $T_y \approx 0$  due to large signal attenuation by absorption [see Eq. (38)]. By application of a control field, the absorption peak ( $\text{Im}\langle s_0^+ \rangle$ ) splits - giving rise to Autler-Townes doublet. The minimum of  $\text{Im}\langle s_c^+ \rangle$  appears at  $\delta \sim 0$ . Thus MOR signal at this frequency is enhanced by suppressing the  $\sigma_-$  component of the probe field as a result of its large absorption. (ii) Further, large MOR signal is observed for a fairly large range of probe frequencies ( $-50 < \delta < 50$ ) - which is attributed to the flipping of the sign of  $\text{Re}\langle s^+ \rangle$  causing a larger asymmetry between  $\text{Re}\langle s_c^+ \rangle$  and  $\text{Re}\langle s_0^- \rangle$ . However large absorption reduces most part of the rotation signal. Hence it is observed that  $T_y$  is maximum ( $\approx 27\%$ ) at  $\delta \approx -50$  when both  $\text{Im}\langle s^- \rangle$  and  $\text{Im}\langle s_c^+ \rangle$  are small.

In Fig. 4, we consider the control of MOR in a denser medium. Here  $\alpha l = 3000$  and the magnetic field is such that  $\zeta = 20$ . In order to demonstrate the combined effect of  $\mathcal{E}_c$  and  $B$ , and then to isolate the contribution of magnetic field in obtaining large  $T_y$ , we have also plotted  $T_y$  for  $B = 0$  but  $\mathcal{E}_c \neq 0$ . In the following we discuss the contribution of  $\mathcal{E}_c$  and  $B$  in different probe frequency regions. To understand the enhancements and suppressions of the MOR signal at different probe frequencies, we analyze the following different regions in Fig. 4 :

*Region I:* For  $-50 < \delta < 50$ ,  $\text{Im}\langle s_0^\pm \rangle$  are large. Thus in the absence of control field,  $T_y$  in this region is almost zero. However by application of control field, an absorption minimum for  $\sigma_-$  polarization component ( $\text{Im}\langle s_c^+ \rangle$ ) occurs due to EIT at  $\delta = 0$ . Thus a large enhancement of MOR is obtained when  $\mathcal{E}_c \neq 0$  compared to the case of  $\mathcal{E}_c = 0$ . However  $T_y$  value is only 10.2% of the input probe intensity at  $\delta = 0$ , because  $\frac{\alpha l}{2} \text{Im}\langle s_0^- \rangle$  still has a large value and therefore

$$T_y \approx \frac{1}{4} \left| e^{i\frac{\alpha l}{2}\langle s_c^+ \rangle} \right|^2 \approx \frac{1}{4} e^{-\alpha l \text{Im}\langle s_c^+ \rangle} \quad (41)$$

is small. This rotation is solely due to *dichroism* created by the control laser. Comparing the  $T_y$  values with  $B = 0, \mathcal{E}_c \neq 0$  (dot-dashed line) and  $B \neq 0, \mathcal{E}_c \neq 0$  (dashed line), it is clear from the Fig. 4 that the magnetic field contribution is very small in this region.

*Region II:* In the region  $-100 < \delta < -50$ , there are residual absorptions at the tail of the Lorentzian  $\text{Im}\langle s_0^\pm \rangle$ . Further  $\text{Im}\langle s_c^+ \rangle$  is also large in this region. Therefore though there is a large asymmetry between  $\text{Re}\langle s_0^- \rangle$  and  $\text{Re}\langle s_c^+ \rangle$ , very large attenuation makes the value of  $T_y$  extremely small.

*Region III:* In the probe frequency region  $-200 < \delta < -100$ , minimum of  $\text{Im}\langle s_0^\pm \rangle$  occurs but  $\text{Im}\langle s_c^+ \rangle$  still has large value in this region. Thus the rotation is large in absence of  $\mathcal{E}_c$  but with the control field, there occurs a large suppression of the MOR signal.

*Region IV:* For  $-300 < \delta < -200$ , we get the most interesting region because the  $\text{Im}\langle s_0^\pm \rangle$  and  $\text{Im}\langle s_c^+ \rangle$  are very small. Thus even though the asymmetry between  $\text{Re}\langle s^\pm \rangle$  is small, the birefringence contribution shows up in the form of very large rotation in this region. For example, the MOR signal at  $\delta = -248.3$  is 86.1% of the input intensity. The comparison of control field induced  $T_y$  in presence and absence of magnetic field clearly demonstrates that the presence of magnetic field causes larger asymmetry between  $\langle s_c^+ \rangle$  and  $\langle s_0^- \rangle$  in this region. For example at  $\delta \approx -300$ ,  $T_y$  with magnetic field is about 5 times larger compared to that without magnetic field. However in the +ve  $\delta$  region ( $200 < \delta < 300$ ), the asymmetry between  $\langle s_0^- \rangle$  and  $\langle s_c^+ \rangle$  is reduced, and hence MOR is suppressed.

In order to bring out the role of magnetic field in the enhancement of  $T_y$  observed in this region, we present Fig. 5(a) - where  $T_y$  vs magnetic field is plotted with a probe frequency fixed ( $\delta = -250$ ) in the region IV. The figure clearly demonstrates the contribution of magnetic field and laser field separately in the enhancement of  $T_y$ . For clarity of

the explanation, we have marked some points in the graph. The point  $A_1$  ( $B_1$ ) represents the rotation due to control field alone with  $G_1 = 100$  ( $G_1 = 50$ ). The points  $A_2$  ( $A_3$ ) gives the amount of  $T_y$  without (with) the control field for a given value of  $\zeta = 22.4$  ( $\zeta = 44.45$ ). Thus clearly,  $A_3$  represents enhancement of rotation by a factor of 2.37 due to the magnetic field with respect to  $A_1$ , and when compared with  $A_2$ , the point  $A_3$  represents enhancement due to the control field by a factor of 2.66. Very large  $T_y$  ( $\approx 86.8\%$  of input intensity) is obtained for  $\zeta = 22.4$ . The plot with  $G_1 = 50$  shows a large  $T_y$  ( $\approx 90.9\%$  of input intensity) value at  $\zeta = 44.54$  which corresponds to an enhancement of  $4.5 \times 10^3$  times the value compared to the point  $B_1$ . Similarly large suppression of MOR can be observed when the magnetic field is flipped (i.e.  $\zeta$  is negative); e.g., the point  $A_4$ . The large MOR signals and enhancements described above are interpreted by the condition (39). *The points where the condition (39) is satisfied are marked by arrows in Fig. 5(b)*. The Fig. 5(b) also depicts the parameters for which the rotations are optimal. From Fig. 5, it may be noted that large  $T_y$  can be produced either by a large magnetic field and a weaker control field, or a weaker magnetic field and a strong control field. This could be advantageous as it is difficult to produce large magnetic fields in laboratory. Further using the large enhancements ( $\eta$ ) of MOR it is possible to realize a *magneto-optical switch*, that can switch the incident polarization of the probe to its orthogonal polarization [27,34].

## VII. MOR IN TWO-PHOTON RESONANCE CONDITION

In this section we consider the enhancement of MOR when the  $\sigma_+$  polarized control field and the probe field are always on two-photon resonance with  $|e\rangle \leftrightarrow |g\rangle$  transition ( $\Delta + \delta = 0$ ). In the following discussion, we consider both the cases of stationary atom and homogeneously broadened atom with the above condition.

### 1. Stationary Atom Case:

For a stationary atom, the susceptibilities are given by Eq. (19) and (20) but with  $\delta_v \rightarrow \delta$ . Under the condition  $\delta + \Delta = 0$ ,  $s_c^+$  (that denotes  $s^+$  in presence of control field) reduces to

$$s_c^+ = \frac{i\gamma}{\left(\frac{|G_1|^2}{\Gamma_o + \Gamma_1 + \Gamma_2} + \gamma\right) + i(\delta + \zeta)}; \quad (42)$$

which is a Lorentzian profile with a width given by  $\left(\frac{|G_1|^2}{\Gamma_o + \Gamma_1 + \Gamma_2} + \gamma\right)$ . The width is too large for a control field  $G_1 \gg \gamma$ , causing large power broadening. Thus for small values of  $\delta + \Omega$ ,  $s_c^+$  is negligibly small. However,  $s^-$  remains unchanged. Therefore  $T_y$  (in Eq.(34)) reduces to

$$T_y = \frac{1}{4} \left| 1 - e^{i\frac{\omega t}{2}} s^- \right|^2; \quad (43)$$

and hence  $T_y$  becomes independent of the control field for  $|G_1| \gg |\delta + \zeta|$ . The  $(T_y)_{max}$  value thus remains same for any arbitrary value of  $\zeta$ ; e.g. for  $G_1 = 20$ ,  $(T_y)_{max} \sim 60\%$  for any  $\zeta$  (results not shown here). However changing the magnetic field, the  $T_y$  structure shifts along  $\delta$  and  $T_y$  curve is symmetric about  $\zeta$ . Therefore by choosing proper magnetic field, one can produce large  $T_y$  and enhancement of  $T_y$  at the required probe frequency regions.

### 2. Doppler Broadened Case:

We further consider the enhancement of MOR in the Doppler broadened medium with the fields  $\mathcal{E}_p$  and  $\mathcal{E}_c$  in two-photon resonance condition, where  $\Delta + \delta = 0$ . Under this condition  $\langle s^+ \rangle$  in Eq. (27) is modified which contains the control field parameters but  $\langle s^- \rangle$  remains unchanged. Further in the limit  $|G_1| \gg \omega_D$ , one can show that  $\langle s^+ \rangle$  becomes equal to the corresponding stationary atom value of  $s^+$  in Eq. (42). However, note that  $\langle s^- \rangle$  [in Eq. (26)] is still velocity dependent. In the above limit, large power broadening is introduced in  $\langle s^+ \rangle$  and amplitude of  $\langle s_c^+ \rangle$  is reduced. However, this turns out to be advantageous, particularly because large asymmetry is created between  $\text{Re} \langle s_c^+ \rangle$  and  $\text{Re} \langle s^- \rangle$  around  $\delta = \zeta$ . Moreover the absorption  $\text{Im} \langle s_c^- \rangle$  becomes extremely small. Since  $\langle s^- \rangle$  is Doppler broadened and  $\langle s_c^+ \rangle$  is reasonably small and flat for a broad range of  $\delta$ , one obtains *large enhancement of  $T_y$  for a broad range of probe frequencies compared to the homogeneously broadened case*. Further, MOR in two-photon resonance condition turns out to be advantageous for smaller magnetic fields where very large enhancement of MOR is obtained.

## VIII. SUMMARY

In summary, we have shown how a control field can be used to control birefringence and hence enhance MOR in a Doppler broadened medium. We have shown how control laser can modify the susceptibilities and hence result significantly large MOR in frequency regions, where MOR otherwise is small. The key to large enhancement of MOR



consists of utilizing the large asymmetry in the susceptibilities caused by the Autler-Townes splitting. We have derived conditions to select frequency regions where one can obtain large MOR. The most useful regions are found to be at the probe frequencies - where absorptions of both the circularly polarized components are negligible and the associated dispersions are quite different. We have substantiated these analytical results using many numerical plots for many different parameters at different conditions. We have also demonstrated the significance of magnetic field and control field in obtaining the large MOR by isolating the effects of the two fields. Finally we have discussed the possibility of large enhancement of MOR for a broad range of probe frequencies - when probe and control fields are in two-photon resonance condition.

- 
- [1] D. S. Kliger, J. W. Lewis, and C. E. Randall, “*Polarized light in optics and spectroscopy*” (Academic Press, 1990).
- [2] J-P Connerade, J. Phys. B **16**, 399 (1983); J-P Connerade, T. A. Stavarakas, and M. A. Baig, *Synchrotron Radiation Sources and their Applications*, ed. G. N. Greaves and I. H. Munro (Edinburgh: SUSSP Publications, Edinburgh University, 1989), p. 310; X. H. He and J-P Connerade, J. Phys. B **26**, L255 (1993).
- [3] W. Gawlik, J. Kowalski, R. Neumann, H. B. Weigemann, and K. Winkler, J. Phys. B **12**, 3873 (1979); X. Chen, V. L. Telegdi, and A. Weis, Opt. Commun. **74**, 301 (1990); E. Pflöghaar, J. Wurster, S. I. Kanorsky, and A. Weis, *ibid* **99**, 303 (1993); A. J. Wary, D. J. Heading, and J-P Connerade, J. Phys. B **27**, 2229 (1994).
- [4] For extensive discussion on MOR and many interesting applications see: J-P. Connerade, *Highly Excited Atoms*, (Cambridge University Press, 1998).
- [5] P. Avan and C. Cohen-Tannoudji, J. Physique Lett. **36**, L85 (1975); S. Giraud-Cotton, V. P. Kaftandjian, and L. Klein, Phys. Rev A **32**, 2211 (1985); F. Schuller, M. J. D. MacPherson, and D. N. Stacey, Opt. Commun. **71**, 61 (1989).
- [6] K. H. Drake and W. Lange, Opt. Commun. **66**, 315 (1988); P. Jungner, T. Fellman, B. Stahlberg, and M. Lindberg, *ibid*, **73**, 38 (1989).
- [7] G. S. Agarwal, P. Anantha Lakshmi, J-P Connerade, and S. West, J. Phys. B **30**, 5971 (1997).
- [8] For a recent review of MOR with laser sources see: W. Gawlik, in “*Modern Non-linear Optics*”, ed. M. Evans, and S. Kielich, Advances in Chemical Physics Series vol. LXXXV, Part 3 (Wiley, New York, 1994).
- [9] M. Yamamoto and S. Murayama, J. Opt. Soc. Am. **69**, 781 (1979).
- [10] F. Schuller, R. B. Warrington, K. P. Zetie, M. J. D. Macpherson, and D. N. Stacey, Opt. Commun. **93**, 169 (1992).
- [11] G. Labeyrie, C. Miniatura, and R. Kaiser, arXiv: physics/0103045.
- [12] A. M. Bonch-Bruevich, N. N. Kostin, and V. A. Khodovoi, JETP Lett. **3**, 279 (1966).
- [13] W. Harper, Prog. Quantum Electron. **1**, 53 (1970).
- [14] P. F. Liao and G. C. Bjorklund, Phys. Rev. Lett. **36**, 584 (1976); Phys. Rev. A **15**, 2009 (1977).
- [15] C. Wieman and T. W. Hänsch, Phys. Rev. Lett. **36**, 1170 (1976); R. Teets, R. Feinberg, T. W. Hänsch and A. L. Schawlow, Phys. Rev. Lett. **37**, 683 (1976).
- [16] Yu. Heller, V. F. Lukinykh, A. K. Popov, and V. V. Slabko, Phys. Lett. **82A**, 4 (1981); see also S. Cavalieri, M. Matera, F. S. Pavone, J. Zhang, P. Lambropoulos, and T. Nakajima, Phys. Rev. A **47**, 4219 (1993).
- [17] B. Ståhlberg, P. Jungner, T. Fellman, K.-A. Suominen, and S. Stenholm, Opt. Commun. **77**, 147 (1990); K.-A. Suominen, S. Stenholm, B. Ståhlberg, J. Opt. Soc. America B **8**, 1899 (1991).
- [18] M. O. Scully, Phys. Rev. Lett. **67**, 1855 (1991).
- [19] M. O. Scully and M. Fleischhauer, Phys. Rev. Lett. **69**, 1360 (1992); Phys. Rev. A **49**, 1973 (1994); M. Fleischhauer, A. B. Matsko, and M. O. Scully, Phys. Rev. A **62**, 013808 (2000).
- [20] V. A. Sautenkov, M. D. Lukin, C. J. Bednar, I. Novikova, E. Mikhailov, M. Fleischhauer, V. L. Velichansky, G. R. Welch, and M. O. Scully, Phys. Rev. A **62**, 023810 (2000); I. Novikova, A. B. Matsko, V. A. Sautenkov, V. L. Velichansky, G. R. Welch, and M. O. Scully, Opt. Lett. **25**, 1651 (2000).
- [21] D. Budker, V. Yashchuk, and M. Zolotarev, Phys. Rev. Lett. **81**, 5788 (1998); D. Budker, D. F. Kimball, S. M. Rochester, and V. V. Yashchuk, Phys. Rev. Lett. **85**, 2088 (2000); D. Budker, D. F. Kimball, S. M. Rochester, V. V. Yashchuk, and M. Zolotarev, Phys. Rev. A **62**, 043403 (2000).
- [22] D. Budker, D. F. Kimball, S. M. Rochester, and V. V. Yashchuk, Phys. Rev. Lett. **83**, 1767 (1999).
- [23] F. S. Pavone, G. Bianchini, F. S. Cataliotti, T. W. Hänsch, M. Inguscio, Opt. Lett. **22**, 736 (1997).
- [24] S. E. Harris, Phys. Today, Pg. 36, July (1997); S. E. Harris, G. Y. Yin, M. Jain, H. Xia, and A. J. Merriam, Philos. Trans. R. Soc. (London) A **355**, 2291 (1997).
- [25] S. Wielandy and A. L. Gaeta, Phys. Rev. Lett. **81**, 3359 (1998).
- [26] A. K. Patnaik and G. S. Agarwal, Opt. Commun. **179**, 97 (2000).
- [27] A. K. Patnaik and G. S. Agarwal, in *Frontiers of Laser Physics and Quantum Optics*, Eds. Z. Xu, S. Xie, S. -Y. Zhu, M. O. Scully (Springer-Verlag, Germany), pg. 403.
- [28] A. D. Cronin, R. B. Warrington, S. K. Lamoreaux, and E. N. Fortson, Phys. Rev. Lett. **80**, 3719 (1998).

- [29] Y. Chen, C. Lin, and I. A. Yu, Phys. Rev. A **61**, 053805 (2000); D. McGloin, M. H. Dunn, and D. J. Fulton, Phys. Rev. A **62**, 053802 (2001).
- [30] M. Xiao, Y. Li, S. Jin, and J. G. Banacloche, Phys. Rev. Lett. **74**, 666 (1995); J. G. Banacloche, Y. Li, S. Jin, and M. Xiao, Phys. Rev. A **51**, 576 (1995); Y. Li and M. Xiao, *ibid* R2730 (1995).
- [31] G. Vemuri and G. S. Agarwal, Phys. Rev. A **53**, 1060 (1996); G. Vemuri, G. S. Agarwal and B. D. N. Rao, *ibid*, 2842 (1996).
- [32] W. Demtröder, *Laser Spectroscopy* (Springer, Berlin, 1998), Chap.3; R. Loudon, *The Quantum Theory of Light* (Oxford University Press), Chap.2.
- [33] M. Abramowitz and I. A. Stegun, *Hand Book of Mathematical Functions*, (Dover Publication, NY, 1972), pg. 279.
- [34] Note that the paper [E. L. Lago and R. de la Fuente, Phys. Rev. A **60**, 549 (1999)] reports polarization switching in a Kerr medium.

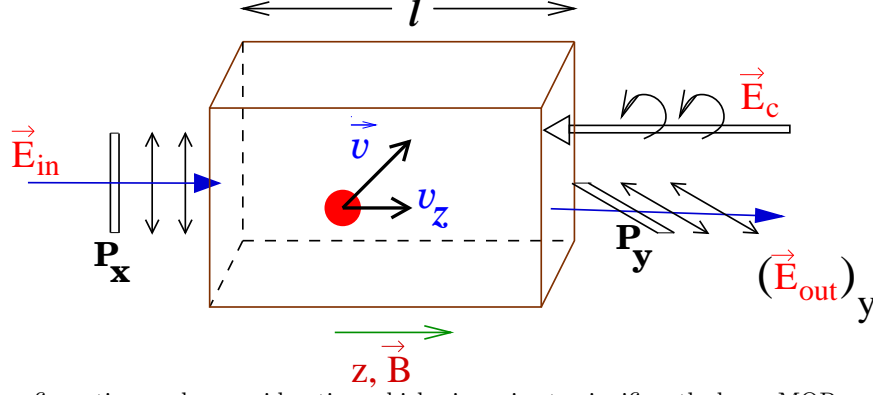


FIG. 1. The configuration under consideration which gives rise to significantly large MOR and large enhancements. The direction of magnetic field  $\vec{B}$  fixes quantization axis ( $z$ -axis). The control field ( $\vec{E}_c$ ) and the input probe field ( $\vec{E}_{in}$ ) are counter propagating along the  $z$ -axis. The atom in the cell moves with velocity  $\vec{v}$  in arbitrary directions.  $P_x$  and  $P_y$  are  $x$ -polarizer at input and  $y$ -polarized analyzer at the output respectively.  $(\vec{E}_{out})_y$  is the output probe after passing through  $P_y$ .

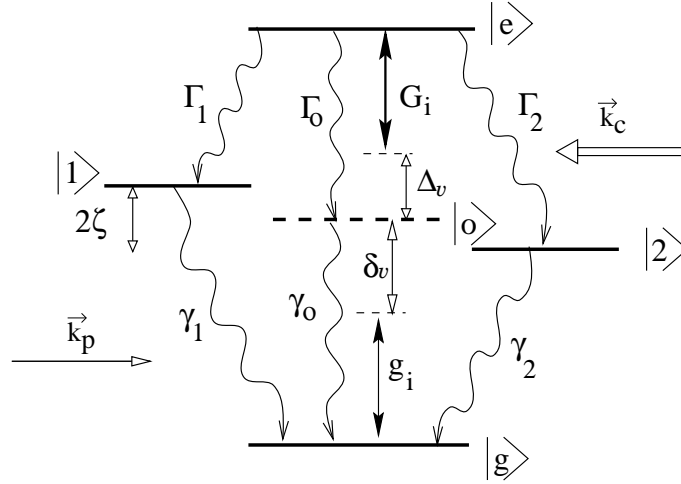


FIG. 2. The four-level model scheme having  $m$ -degenerate sub-levels  $|1\rangle$  and  $|2\rangle$  as its intermediate states. The magnetic field  $\vec{B}$  gives rise to Zeeman splitting  $2\zeta$ . The spontaneous decay rates are denoted by  $2\Gamma_i$  and  $2\gamma_i$ . The probe field ( $\vec{k}_p$ ) and the control field ( $\vec{k}_c$ ) are counter propagating. The Rabi frequencies of the probe field and the control field are given by  $2g_i$  and  $2G_i$ , corresponding to the  $|i\rangle \leftrightarrow |g\rangle$  and  $|e\rangle \leftrightarrow |i\rangle$  couplings respectively ( $i = 1, 2$ ). The detunings of the probe and the control fields from the degenerate  $j = 1$  state, in the moving atomic frame of reference, are  $\delta_v$  and  $\Delta_v$  respectively.

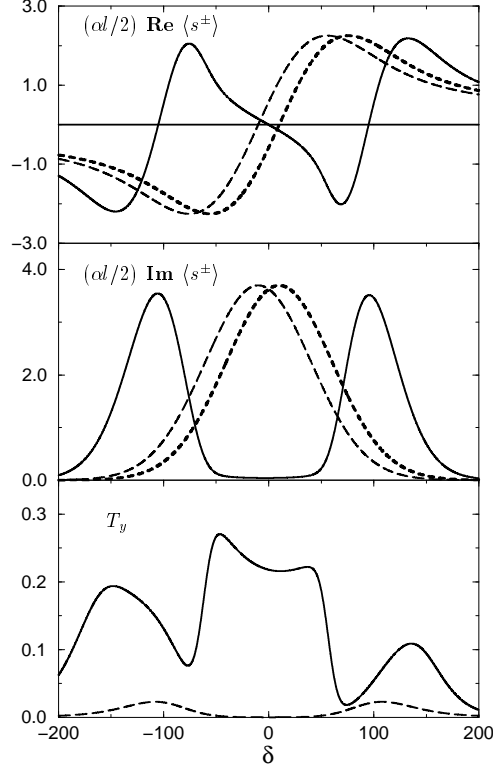


FIG. 3. The enhancements of MOR for a control field tuned to  $|e\rangle \leftrightarrow |o\rangle$  transition ( $\Delta = 0$ ) with Rabi frequency  $G_1 = 100$ . In the plots for  $\frac{\alpha l}{2} \langle s^\pm \rangle$ , the thick-dashed (long-dashed) lines represent  $\frac{\alpha l}{2} \langle s_0^- \rangle$  ( $\frac{\alpha l}{2} \langle s_0^+ \rangle$ ) and solid lines represent  $\frac{\alpha l}{2} \langle s_c^+ \rangle$ . In the plot for  $T_y$ , dashed (solid) curve represents the rotation without (with) control field. The other parameters used are  $\omega_D = 50$ ,  $\zeta = 10$  and  $\alpha l = 300$ . All frequencies are scaled with  $\Gamma_o = \Gamma_1 = \Gamma_2 = \gamma$ .

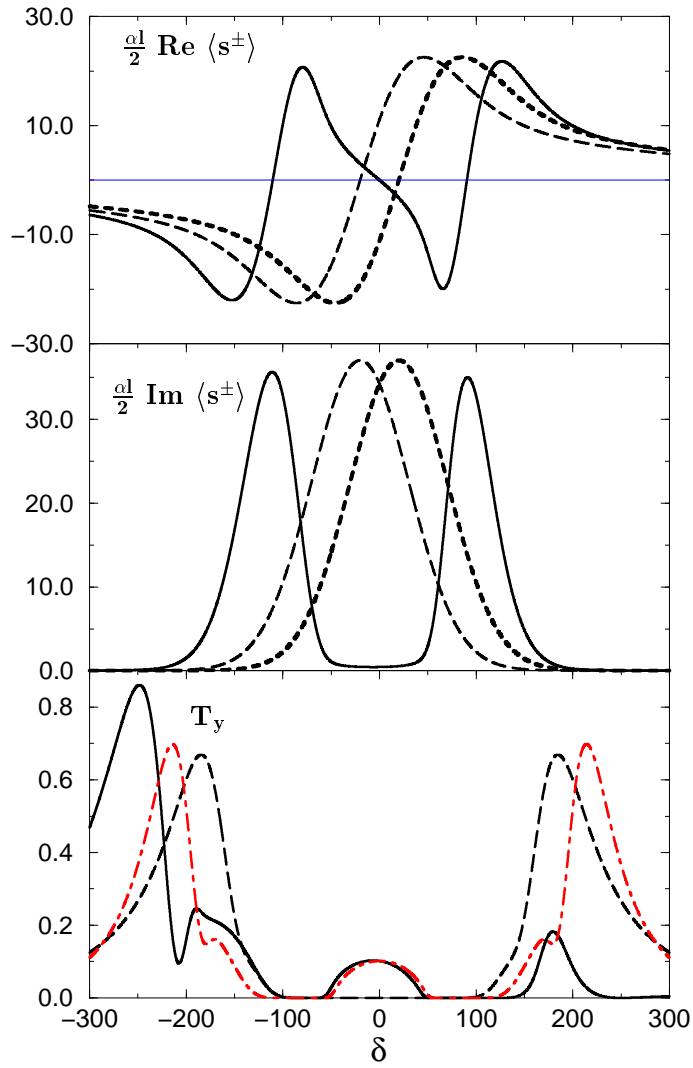


FIG. 4. Enhancement and suppression of MOR in a denser medium with  $\alpha l = 3000$ . The legends of the curves used are same as in Fig. 3. The magnetic field used in this plot is  $\zeta = 20$ , the control field Rabi frequency is taken to be  $G_1 = 100$  and the Doppler width is  $\omega_D = 50$ . A plot of  $T_y$  with  $\zeta = 0$  but with  $\mathcal{E}_c \neq 0$  (dot-dashed line in the plot for  $T_y$ ) is also presented to isolate the roles of  $\mathcal{E}_c$  and  $B$  in controlling the MOR. All frequencies are scaled with  $\Gamma_o = \Gamma_1 = \Gamma_2 = \gamma$ .

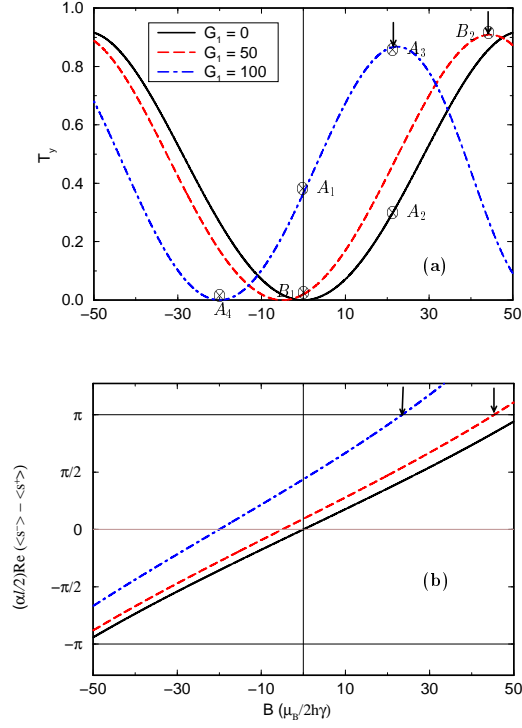


FIG. 5. (a) The plot of  $T_y$  as a function of  $B$  to investigate the role of magnetic field. This plot corresponds to  $\delta = -250$  (in the region IV of Fig. 4). All other parameters are same as in Fig. 4. (b) The asymmetry between  $\langle s^+ \rangle$  and  $\langle s^- \rangle$  is plotted as a function of  $B$  corresponding to the plots of  $T_y$  in (a). The points marked by the arrows satisfy the condition for maximal rotation (39).

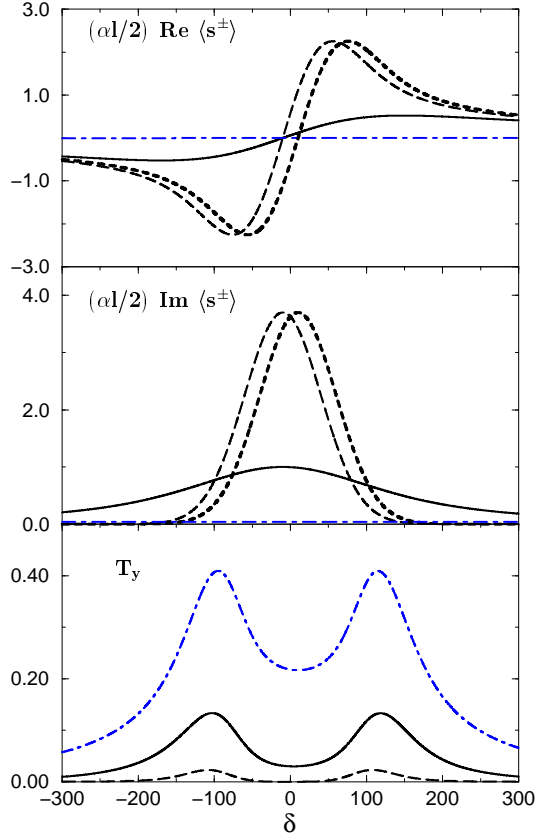


FIG. 6. Enhancement of MOR in a Doppler broadened medium when the control field and the probe field are on two-photon resonance with  $|e\rangle \leftrightarrow |g\rangle$  transition. The legends used are same as in Fig. 3, the solid line corresponds to  $G_1 = 20$  and the dot dashed line corresponds to  $G_1 = 100$ . Here  $G_1 = 100$  corresponds to the limit where  $\langle s_c^+ \rangle$  becomes equal to  $s^+$  in (42). The other parameters used in the plot are  $\zeta = 10$  and  $\alpha l = 300$ .